vertical measurements. Also, the time taken by the different stochastic methods is compared. The longer data spans give reliable results as well as less standard deviation for residuals. Using the single-frequency receiver, the standard deviation of the residuals is the same for all three stochastic methods. The MINQUE model gives more reliable results than the other two procedures and requires high computational time. The simplified MINQUE method gives equivalent results with comparatively low computational time. MINQUE and simplified MINQUE methods give better results in standard deviation of residuals compared to the standard stochastic model, particularly for the vertical measurement of the residuals. Hence deformation-monitoring studies related to mining subsidence or landslides should be analysed using the MINQUE or simplified MINQUE methods.

1. Hoffmann-Wellenhof, B., Lichtenegger, B. and Collins, J., *GPS Theory and Practice*, Springer-Verlag, New York, 2001, 5th edn, pp. 201; 214–217; 249; 258–264.
2. Wang, J., Stewart, M. P. and Tsakiri, M., Stochastic modeling for static GPS baseline data processing. *J. Surv. Eng.*, 1998, **72**, 171–181.
3. Rao, C. R., Estimation of variance and covariance components – MINQUE theory. *J. Multivariate Anal.*, 1971, **1**, 112.
4. Satirapod, C., Wang, J. and Rizos, C., A simplified MINQUE procedure for the estimation of variance–covariance components of GPS observables. *Surv. Rev.*, 2002, **36**, 582–590.
5. Satirapod, C., Wang, J. and Rizos, C., A new stochastic modeling procedure for precise static GPS positioning. *Z. Vermessungswes.*, 2001, **126**, 365–373.
6. Satirapod, S., Improving the GPS data processing algorithm for precise static relative positioning. Ph D thesis, School of Surveying and Spatial Information Systems, The University of New South Wales, Sydney, Australia, 2002.
7. Wang, J., Stewart, M. P. and Tsakiri, M., A discrimination test procedure for ambiguity resolution on-the-fly. *J. Geodesy*, 1998, **72**, 644–653.
8. Wang, J., Stewart, M. P. and Tsakiri, M., A comparative study of the ambiguity validation procedures. *Earth Planet Space*, 2000, **52**, 813–817.
9. Teunissen, P. J. G., The least-squares ambiguity decorrelation adjustment: A method for fast GPS integer ambiguity estimation. *J. Geodesy*, 1995, **70**, 65–82.
10. Joosten, P. and Tiberius, C. C. J. M., *Mathematical geodesy and positioning*, Delft University of Technology, The Netherlands, 2002, vol. 6, pp. 109–114.

Received 19 February 2007; revised accepted 7 September 2007

Ground-penetrating radar investigation along Pinjore Garden Fault: Implication toward identification of shallow subsurface deformation along active fault, NW Himalaya

J. N. Malik*, A. K. Sahoo and A. A. Shah

Department of Civil Engineering, Indian Institute of Technology, Kanpur 208 016, India

A total of 24 m Ground Penetrating Radar (GPR) profiles acquired across the 6 m high Pinjore Garden Fault (PGF) scarp with 200 MHz antenna, yielded high-resolution subsurface image with penetration depth up to 6 m. Two strands of low-angle thrust faults (F1 and F2) were identified based on the prominent offset and warping in radar reflections. The F1 fault strand in the GPR profile was consistent with the fault identified in the trench excavated across the PGF. The GPR profile helped us to trace the fault strand of F1 at greater depth (>3 m) than that identified in the trench and also a new trace of fault branch F2 in the upper portion of the scarp. This suggested that multiple events have occurred along the PGF during the recent geologic past. With this attempt we suggest that the GPR technique can be a useful tool in mapping the shallow subsurface geometry and in locating the near-surface faults displacing young Quaternary sediments in the Himalayan foothill zone.

Keywords: Active fault, ground-penetrating radar, shallow subsurface geometry.

THE Himalayan mountain range is a result of the collision between the Indian and Eurasian plates. The northward convergence of the Indian plate keeps the entire Himalayan arc seismically active, which is responsible for the occurrence of large and moderate magnitude earthquakes. In the recent past, the Himalaya has experienced three large-magnitude earthquakes: 1905 Kangra (M_w 7.8), 1934 Bihar (M 8.4) and the 1950 upper Assam (M 8.5)[1,2]. Besides these, the 8 October 2005 Muzaffarabad earthquake (*Mw* 7.6) occurred along an active fault which was earlier identified as the Tanda Fault[3–5]. Therefore, identification of active faults bears significant importance in recognizing the seismic potential and assessing their associated seismic hazards in the Himalayan terrain. For proper seismic hazard estimation, it is necessary to know the accurate locations and geometries of active faults, including those hidden beneath young sediment cover[6].

Palaeoseismic investigation is one of the most commonly adopted techniques towards identification/cataloguing of the historic and pre-historic earthquakes in tectonically

*For correspondence. (e-mail: javed@iitk.ac.in)

active regions of the world[7]. It has also been realized that due to rapid deposition or degradation the tectonic landforms are buried, making it difficult in identifying adequate sites to undertake palaeoseismic investigations[8]. With such constraints, several studies using geophysical methods like seismic reflection and seismic refraction, have been carried out to map and understand the pattern of shallow subsurface deformation along the active zones. These geophysical methods give good vertical resolution in terms of depth of about ≥ 100 m, but the sub-metre resolution is not satisfactory. Consequently, during the mid 1990s, the Ground Penetrating Radar (GPR) technique was extremely useful in the field of geology, as it can give a high-resolution profile of shallow subsurface succession up to sub-metre resolution[9].

In recent years, the GPR technique has been used for mapping the shallow sub-surface deformation in the young Quaternary sediments, for identifying neotectonic faulting activity and liquefaction features like sand-blows[6–18]. Along with this it has also been used in mapping subtle sedimentation pattern[9,19] and in locating archeological sites[20,21]. This technique has been found to be effective in identifying the most appropriate site for trenching to conduct detailed palaeoseismic studies along active faults[6,8]. The GPR survey along the San Andreas Fault (SAF), North California revealed two SAF strands based on vertically displaced prominent georadar reflections; it was also suggested after comparing the data with the trench section that these strands were probably generated by the 1906 San Francisco earthquake and/or earlier events[15]. GPR investigation conducted in Japan across the well-known Uemachi Fault System (UFS) helped in identifying the geometry of a subsurface fault scarp that had a visible expression at the surface along with several subsurface fault strands associated with the UFS[16]. Similar studies in Taiwan helped in delineating the subsurface pattern and palaeoseismic facies of the active Chihshang Fault[12].

Here we report the results of GPR investigation made across the Pinjore Garden Fault (PGF) scarp (Figure 1 *a* and *b*) to work out the following issues: (i) Whether the GPR technique is capable of mapping the shallow subsurface geometry and location of the shallow subsurface deformation in Himalayan foothill zone? (ii) Are there any hidden PGF strands still to be discovered? Apart from a few reports, little information is available from the NW Himalayan region related to the occurrence and distribution of active faults[22–24]. Also, till date no geophysical technique like GPR has been used to locate or map near subsurface deformation along the active faults in the Himalayan foothills. This is our first attempt towards identification of shallow subsurface deformation using GPR in the NW Himalayan foothill zone (Figure 1 *a* and *b*).

The terrain around the study area can be divided into four major geomorphic zones[22,23] from north to south: (i) uplands comprising Lower Siwalik/Lower Tertiary rocks of the Dagshai, Kasauli and Subathu formations; (ii) longitudinal alluvial fill-depression, the Pinjore Dun; (iii) isolated Upper Siwalik frontal range, and Indo-Gangetic Plains (Figure 1 *a*).

In the NW Himalaya, around Chandigarh and Pinjore Dun several active faults like the Chandigarh Fault (CF), Pinjore Garden Fault (PGF), Barsar Thrust and Taksal Fault have been identified[22–25]. These active faults are manifested by well-developed WSW and SW facing fault scarps ranging in height from 5 to 50 m. Among these faults, the PGF extending laterally for more than 45 km NNW–SSE across the Pinjore Dun, has vertically displaced and back tilted the coalesced alluvial fan and alluvial fill deposits, giving rise to WSW and SW-facing fault escarpments[23] ranging in height from 2 to 16 m. These sediments are of late Pleistocene to Holocene age overlying the Middle as well as Lower Siwalik succession[23]. At Ratpur village, the PGF has displaced the Pinjore surface resulting in a well-developed SW facing scarp. Topographic profiling across the 6 m high fault scarp is marked with two prominent breaks, which suggests the occurrence of more than one event[25]. Based on the surface morphology, i.e. degree of dissection of the surface, it has been suggested that this scarp is quite young (late Holocene?) and has preserved the youngest movement along the PGF[23,25]. Besides, a trench excavated at Ratpur village reveals the occurrence of at least two events along a single, low-angle thrust fault (~30°) during the recent past[25].

The GPR is a non-destructive geophysical method that produces a cross-sectional image called the radargram of the shallow subsurface profile up to 50 m depth[9,13]. In recent years several GPR studies have been carried out for mapping near subsurface deformation to assess the geological hazards associated with shallow ruptures[6,8,11–19]. Keeping this in mind, GPR survey was conducted across the PGF scarp in the NW Himalaya foothill zone (Figure 1 *b*).

Data were collected in common-offset continuous mode using portable SIR 3000 single channel system (Geophysical Survey System Inc., USA). While taking the profiles, the antenna was connected with a calibrated odometer fixed on the survey-wheel. Initially attempts were made using 100 and 200 MHz frequency shielded antennas with variable settings to determine the best acquisition parameters. Data collected with 100 MHz antenna gave greater penetration depth than 200 MHz antenna, but data collected with 200 MHz antenna were of higher resolution. Several profiles (striking NE–SW) were collected with 200 MHz, antenna with parameters as listed in Table 1. Besides these parameters, appropriate gain and IIR (Infinite Impulse Response) filter were applied in the field to get better resolution and to remove noise with lower and higher frequencies respectively. The 24 m long GPR profile across the PGF scarp gave penetration depth of about 6 m (Figure 2 *a*).

The radar profile was processed with RADAN 6.5 software by (Geophysical Survey Systems, Inc.). Processing

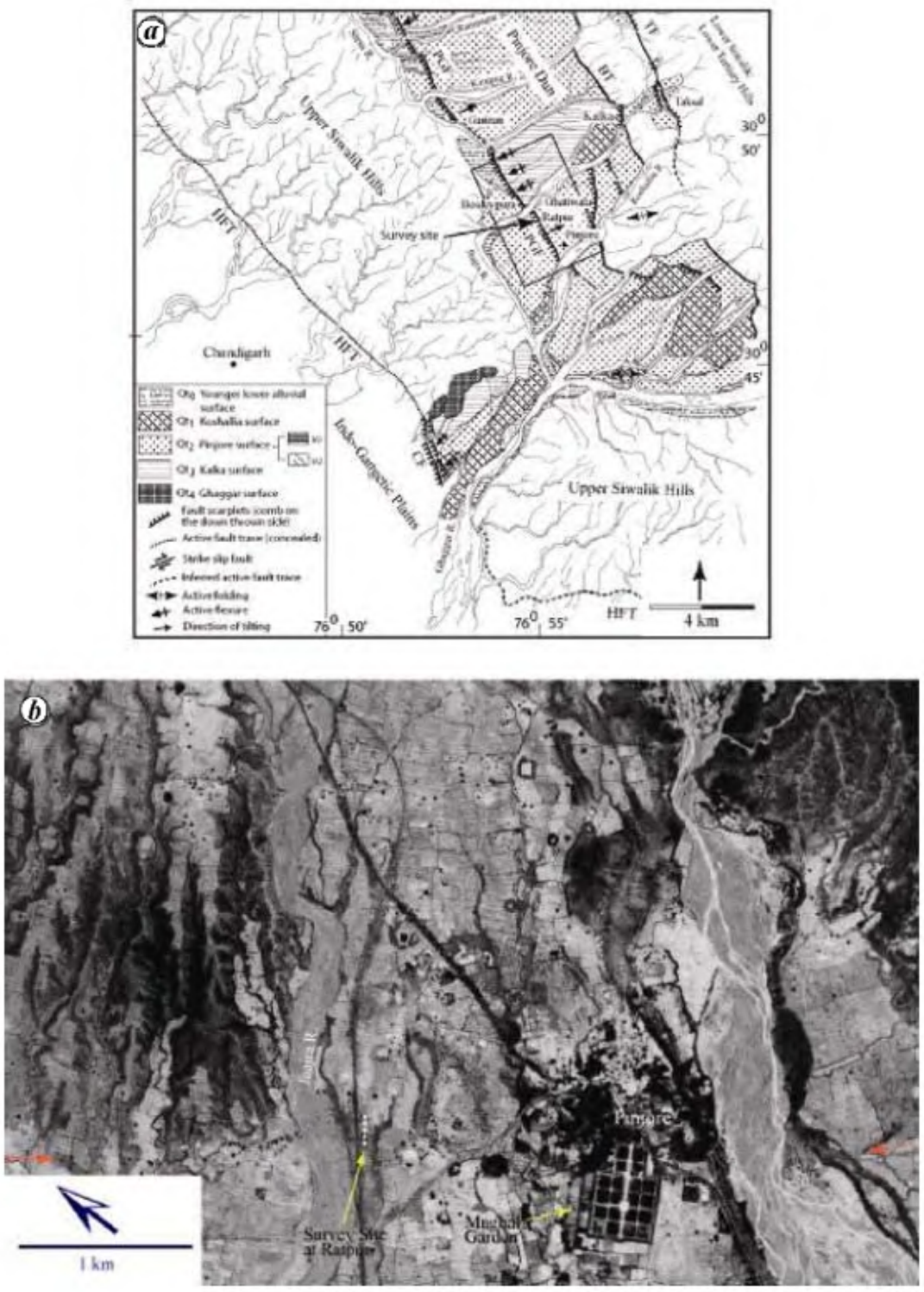

Figure 1. ***a***, Distribution of active fault traces and terraces along northwestern Himalayan foothill zone around Chandigarh and Pinjore Dun. CF, Chandigarh Fault; HFT, Himalayan Frontal Thrust; PGF, Pinjore Garden Fault; BT, Barsar Thrust and TF, Taksal Fault[23]. (Box) Area covered in the satellite photo. Survey site near Ratpur village is shown by arrow. ***b***, Satellite photo showing overall landscape of the area around Ratpur in Pinjore Dun. Active fault traces marked by red arrows cut across different fluvial surfaces along its strike. The PGF trending NW passes through the Mughal Garden.

of the profile was done following appropriate steps (see Table 2). To get proper ground surface and reliable depth, time zero correction was performed, where the uppermost high-amplitude reflections obtained from direct air wave

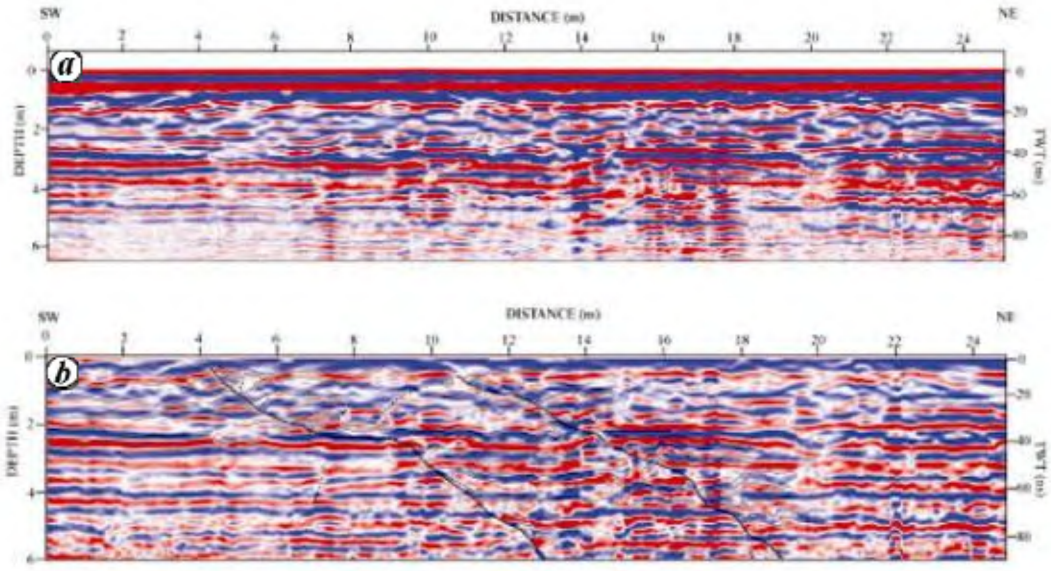

Figure 2. ***a***, Unprocessed 24 m long GPR profile collected across the PGF scarp, which yielded penetration depth up to 6 m. Data are shown in the form of linescan which represents the amplitudes, where red is the positive pulse and blue the negative pulse. ***b***, GPR profile after processing. Two fault strands (F1 and F2) were identified between 4 and 13, and 10 and 20 horizontal distance markers, respectively. The georadar reflector layers are clearly marked by slight warping on the hanging wall-side of both faults. Based on their geometry both faults have been categorized as thrust faults dipping towards NE. Main strands F1 and F2 are marked by thick black lines; thin lines are traces of the different radar reflectors and dashed lines show the inferred subordinate faults. The profile was also compared with the available trench section[25].

Table 1. Acquisition parameters for GPR survey across Pinjore Garden Fault, NW Himalaya

Acquisition parameters	GPR survey
Antenna	200 MHz
Sample/scan	512
Bits/sample	16
Rate (scans/s)	64
Scans/m	100
Infinite impulse response filter	Low pass – 600 MHz High pass – 30 MHz
Dielectric constant	4

Table 2. Data processing sequence and parameters for GPR profile collected across Pinjore Garden Fault

Data processing sequence	
Time zero correction	Removal of high amplitude reflections direct air wave and ground wave
Band pass filter	Low pass – 300 MHz High pass – 40 MHz
Auto gain control	4 points
Topographic correction	
Stacking	

and ground wave were removed (Figure 2 *a* and *b*). For depth conversion we used the available step embedded in the RADAN software. Along with this the profile was also correlated with the available trench section. As the GPR data are usually associated with both low frequency and high frequency noises, to remove such noise, band-pass filters have been designed to pass the signal and reject noise of certain frequencies[10]. Therefore, to remove noise, the FIR (Finite Impulse Response) filter was used (Table 2). Further, to compensate loss in amplitude at depth, slight auto gain control was applied to increase the display resolution (Figure 2 *b*). It is well established that the GPR profile collected across a sloping surface (fault scarps) significantly distorts the subsurface image; hence topographic corrections are required[9]. Therefore, topographic data collected[25] in the field were incorporated in the GPR profile for making topographic correction, followed by surface normalization, so as to get the complete display (Figure 3 *a*). Then stacking was applied to avoid stretching of the data due to topographic correction.

Several studies conducted to map shallow subsurface faulting in Quaternary deposits suggest that the faults on the GPR profile can be recognized by offset of radar reflectors on both sides of the fault strand and warping of the GPR reflectors[6,8,12,15,16]. Taking the above points into consideration for proper interpretation and understanding, we also compared our GPR profile with trench data across the PGF[25].

In the GPR profile, we were able to identify two faults (F1 and F2) strands dipping towards NE (Figures 2 *b* and 3 *a*). Strand F1 was well revealed between the 4 and 13 m horizontal distance marker. We were able to trace this fault up to a depth of 6 m. The georadar reflector layers are

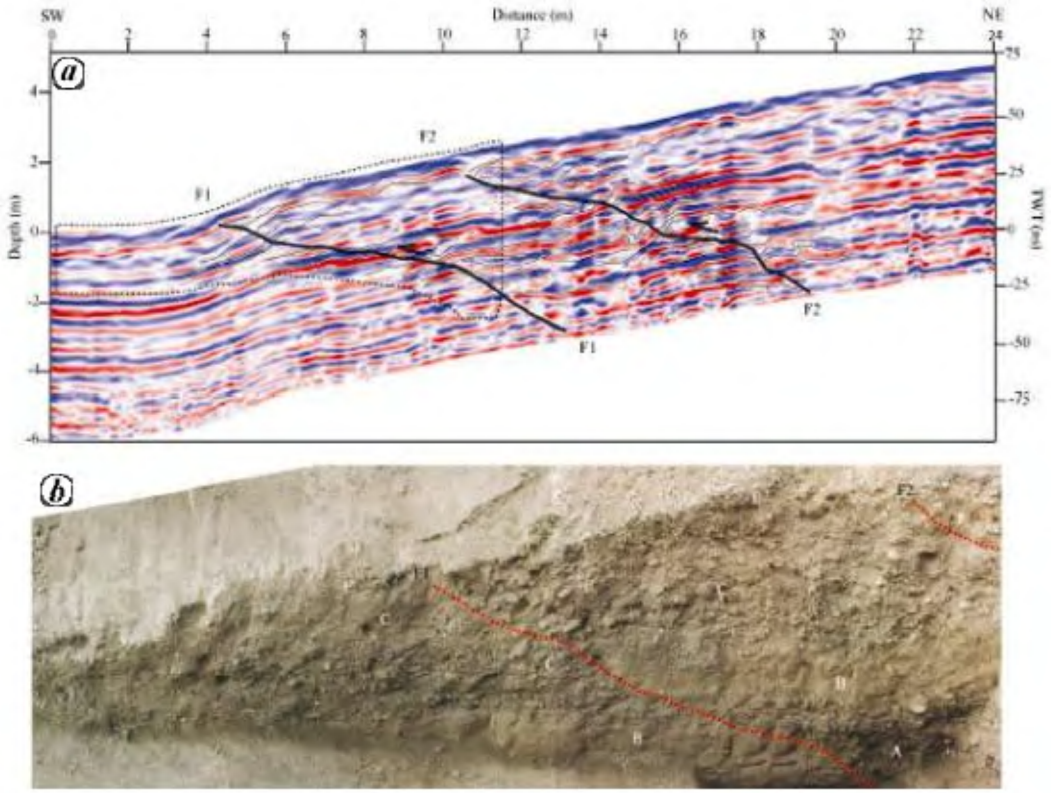

Figure 3. ***a***, Processed GPR profile after topographic correction along with surface normalization and stacking. The identified fault strands are indicated by solid lines between the distance markers 4–13 m and 10–20 m. Box with dotted line shows approximate trench area. ***b***, Northwall view of trench excavated across PGF at Ratpur[25]. The exposed sediment succession in the trench shows units A and C – channel-fill deposits, comprising moderately sorted matrix-supported pebble–cobble–boulder clasts; unit B – massive sand; Unit D – comprising medium to fine gravel and unit E – topsoil. The thrust fault F1 exposed in the trench has displaced lithounits A–C along it. The fault plane dip is variable; it is steep near the surface, becomes gentle in the middle portion and becomes steep again in deeper section. The F1 fault strand is consistent with the trace identified in the GPR profile. Only the tip of the F2 strand was traceable in the upper right corner of the trench, where the fault plane is marked between massive sand (unit F) and gravel (unit C). Fault strands are indicated by red broken lines.

marked by prominent warping close to the surface on the hanging-wall side of the F1 strand, whereas they are horizontal to sub-horizontal towards the southwestern side on the footwall block. This suggests the phenomenon of folding-associated faulting along the F1 strand. Along with this, subordinate back thrust was also observed on the hanging wall block between the 8 and 10 m distance markers. Geometry of the F1 strand was variable; it was marked by a slight high angle near the surface between 4 and 6 m and showed gentle angle between 6 and 10 m, and again become steeper with greater depth between 11 and 14 m. The F1 strand was compared with the trench section, which was found to be consistent (Figure 3 *a* and *b*). As limited section was exposed in the trench[25], we were only able to trace and compare the F1 strand up to 4.5 m of depth and the tip of the F2 strand in the trench. The radar profile helped us in tracing the F1 strand deeper up to the depth of 6 m. The F2 strand between 10 and 19 m horizontal distance markers in the GPR profile revealed a similar pattern of deformation as observed along the F1 strand. The geometry was also similar to the F1 strand, marked by steep fault plane near the surface, which became gentle as one moved deeper and steeper towards the basal portion. This fault (F2) was also traceable up to the depth of 6 m. Since both the fault strands (F1 and F2) cut the radar reflectors close to the surface, it is suggested that the recent movement has been registered along both the faults. The geometry and inclination of the F1 and F2 strands towards NE indicated that these are the branching-out faults, which probably merge with the seismogenic layer at greater depths towards NE.

Our attempt using GPR technique towards mapping shallow subsurface deformation related to active faulting in young Quaternary deposits (Holocene) successfully worked in a dynamic Himalayan foothill zone. The sediment succession in the Himalayan foothill zone, mainly dominated by medium-to-coarse sand–silt, and stratified gravel and sandy lithounits, provided an ideal condition of contrasting sediment-size variation. This sediment condition was ideal in getting prominent radar reflections.

The displacement caused by faulting in this sediment succession was clearly peaked up by GPR profiling across the PGF. The GPR profile collected using a 200 MHz antenna revealed the existence of two strands F1 and F2; the pattern of deformation and fault geometry represents the recent faulting along low-angle thrust faults. The profile was comparable with the available trench section across the PGF from the same site[25], which provided added advantage to our interpretations. The GPR data not only helped in identifying the new fault (F2), but also enabled us to trace the fault (F1) at greater depth, up to 6 m compared to the fault trace identified in the trench[25].

It is therefore suggested that this technique is useful in the Himalayan foothill zone to map the pattern of shallow subsurface deformation and in precisely locating suitable sites for further detailed palaeoseismic investigations along active faults.

1. Ambraseys, N. and Bilham, R., A note on the Kangra *Ms* = 7.8 earthquake of 4 April 1905. *Curr. Sci.*, 2000, **79**, 45–50.
2. Bilham, R., Gaur, V. K. and Molnar, P., Himalayan seismic hazard. *Science*, 2001, **293**, 1442–1444.
3. Kaneda, H. *et al.*, Extensive surface fault rupture associated with the 2005 *Mw* 7.6 Pakistan earthquake. Abstr., In Third Annual Meeting AOGS, Singapore, 2006.
4. Yeats, R. S. and Hussain, A., Surface features of the *Mw* 7.6, 8 October 2005 Kashmir earthquake, northern Himalaya, Pakistan: Implications for the Himalayan front. Abstr., Seismological Society of America, 2006.
5. Nakata, T., Tsutsumi, H., Khan, S. H. and Lawrence, R. D., *Active Faults of Pakistan; Map sheets and Inventories*. Research Center for Regional Geography, Hiroshima University, Special Publication, 1991, vol. 21, p. 144.
6. Gross, R., Green, A., Holliger, K., Horstmeyer, H. and Baldwin, J., Shallow geometry and displacement on the San Andreas Fault near Point Arena based on trenching and 3-D georadar surveying. *Geophys. Res. Lett.*, 2002, **29**, 34-1–34-4.
7. McCalpin, J. P., *Paleoseismology*, Academic Press, New York, 1996, p. 588.
8. Anderson, K. B., Spotila, J. A. and Hole, J. A., Application of geomorphic analysis and ground-penetrating radar to characterization of paleoseismic sites in dynamic alluvial environments: An example from southern California. *Tectonophysics*, 2003, **368**, 25–32.
9. Neal, A., Ground-penetrating radar and its use in sedimentology: Principles, problems and progress. *Earth Sci. Rev.*, 2004, **66**, 261–330.
10. Dobrin, M. B. and Savit, C. H., *Introduction to Geophysical Prospecting*, McGraw-Hill, 1988, p. 867.
11. Bano, M., Marquis, G., Niviere, B., Maurin, J. C. and Cushing, M., Investigating alluvial and tectonic features with ground penetrating radar and analyzing diffraction patterns. *J. Appl. Geophys.*, 2000, **43**, 33–41.
12. Chow, J., Angelier, J., Hua, J. J., Lee, J. C. and Sun, R., Palaeoseismic event and active faulting: From ground penetrating radar and high resolution seismic reflection profile across the Chihshang Fault, eastern Taiwan. *Tectonophysics*, 2001, **333**, 241–259.
13. Audru, J. C., Bano, M., Begg, J., Berryman, K., Henryys, S. and Niviere, B., GPR investigations on active faults in urban areas: The Georisc-NZ project in Wellington, New Zealand. Comptes Rendus de l'Acade´mie des Sciences-Series IIA. *Earth Planet. Sci.*, 2001, **333**, 447–454.
14. Liu, L. and Li, Y., Identification of liquefaction and deformation features using ground penetrating radar in the New Madrid seismic zone, USA. *J. Appl. Geophys.*, 2001, **47**, 199–215.
15. Green, A., Gross, R., Holliger, K., Horstmeyer, H. and Baldwin, J., Results of 3-D georadar surveying and trenching the San Andreas fault near its northern landward limit. *Tectonophysics*, 2003, **368**, 7–23.
16. Rashed, M., Kawamura, D., Nemoto, H., Miyata, T. and Nakagawa, K., Ground penetrating radar investigations across the Uemachi fault, Osaka, Japan. *J. Appl. Geophys.*, 2003, **53**, 63–75.
17. Gegenleitner, R., Hinsh, R., Bruckl, E., Decker, K. and Roch, K. H., Locating neotectonic faults by GPR and reflection seismics. Abstr., European Geophysical Society, vol. 5, 09050.
18. Liberty, L. M., Hemphill-Haley, M. A. and Madin, I. P., The Portland Hills Fault: Uncovering a hidden fault in Portland: Oregon using high-resolution geophysical methods. *Tectonophysics*, 2003, **368**, 89–103.
19. Busby, J. P. and Merritt, J. W., Quaternary deformation mapping with ground penetrating radar. *J. Appl. Geophys.*, 1999, **42**, 75–91.
20. Sternberg, B. K. and McGill, J. W., Archaeology studies in southern Arizona using ground penetrating radar. *J. Appl. Geophys.*, 1995, **33**, 209–225.
21. Whiting, B. M., McFarland, D. P. and Hackenberger, S., Three-dimensional GPR study of a prehistoric site in Barbados, West Indies. *J. Appl. Geophys.*, 2001, **47**, 217–226.
22. Nakata, T., Geomorphic history and crustal movements of foothills of the Himalaya. Report, Tohoku University, Japan, 1972, p. 77.
23. Malik, J. N. and Nakata, T., Active faults and related Late Quaternary deformation along the northwestern Himalayan Frontal Zone, India. *Ann. Geophys.*, 2003, **46**, 917–936.
24. Malik, J. N., Nakata, T., Philip, G. and Virdi, N. S., Preliminary observations from trench near Chandigarh, NW Himalaya and their bearing on active faulting. *Curr. Sci.*, 2003, **85**, 1793–1798.
25. Malik, J. N. and Mathew, G., Evidence of Paleoearthquakes from trench investigations across Pinjore Garden fault in Pinjore Dun, NW Himalaya. *J. Earth Syst. Sci.*, 2005, **114**, 387–400.

ACKNOWLEDGEMENTS. Financial support provided to J.N.M. by DST, New Delhi (DST/23(411)/SU/2003) is acknowledged. We thank Prof. M. Meghroaui, Institute de Physique de Globe de Strasbourg, France, for valuable discussions and suggestions during this study. We thank the reviewers for valuable and constructive comments as well as suggestions which helped in improving the manuscript. We also thank Prashant Mishra and Arvind Pandey for help during this work.

Received 11 August 2006; revised accepted 6 September 2007